ARTICLE

Importance of Metal Cations and Water for Stability of MnO₂ Crystals

Zhi-gang Wei[a,b*], Jia-hong Yan[a], Yang Wu[c], Yue Liu[a]

a. School of Chemical Engineering and Light Industry, Guangdong University of Technology, Guangzhou 510006, China
b. Institute of Theoretical Chemistry, Jilin University, Changchun 130023, China
c. College of Chemistry, Liaoning University, Shenyang 110036, China

Metal cations as well as water are important factors to control the synthesis of MnO₂ crystal nanostructures. In this work, systemic Density functional theory calculations about α, β, δ-MnO₂ are presented to show the importance of metal cations and water for the structure stability and energy stability of MnO₂. It is shown that the α-MnO₂ crystal and its (110) surface will crash without the tunnel cations such as K⁺, and the distance between the layers of the δ-MnO₂ will be significantly lower than that of the experimental results without the interlayer metal cations and water. At the same time, α-MnO₂ and δ-MnO₂ can be more stable than β-MnO₂ with metal cations and water, and vice versa.

Key words: MnO₂, Density functional theory, Metal cation, Formation energy, Structure simulation

I. INTRODUCTION

MnO₂ is a very useful material. It has more than 30 different crystal structures [1, 2], and can act as electrode, supercapacitor, catalyst, ion sieve, adsorbent, etc. [3−7]. In recent years, we tried to control the synthesis of nanostructured manganese oxide with different forms such as α, β, γ, δ, and improve their catalytic properties [8−12]. Based on these researches, we found that metal cations as well as water are important factors to control the synthesis of MnO₂ crystal nanostructures. For example, by using MnSO₄ and KClO₃ as starting materials under hydrothermal conditions, when there are sufficient K⁺ and H⁺, α-MnO₂ is the product; when there is no K⁺ and H⁺, γ-MnO₂ is the product; when there is only H⁺, β-MnO₂ is the product; when there is no H⁺ but Ac⁻, MnOOH is the product [8]. It is obvious that metal cations and water are necessary to prevent collapse for large framework MnO₂ such as romanechite, todorokite, etc. [1]. In fact, these phenomena have alrealy been reported. In 1998, Fritsch et al. reported that the cations in the crystal tunnels were very important for the stability of MnO₂ crystals and without the tunnel cations large framework MnO₂ can not possibly be prepared [13]. In 2006, Johnson et al. demonstrated that the interlayer water is strongly bound to the interlayer cations, and plays an important role in the thermal stability of layered MnO₂ structures [14].

To my knowledge, there has not been a systemic theoretical study about the structure stability and energy stability of MnO₂, which corresponds to the metal cations and water in it. In the present work, we just take the framework α-MnO₂ (2×2 tunnel with metal cation K⁺), β-MnO₂ (1×1 tunnel without metal cation), and layer structure δ-MnO₂ (1×∞ with and without metal cations and water) as examples to show the importance of the metal cations and water by the density functional theory (DFT) calculations.

II. METHODS

The calculations have been performed with DFT with periodic boundary conditions [15]. The exchange-correlation interaction is treated within the generalized gradient approximation (GGA) with the functional parameterized by Perdew, Burke and Enzerhof (PBE) [16]. Atomic basis sets are applied numerically in terms of a double numerical plus polarization function with a global orbital cutoff of 4.7 Å [17]. The geometry optimization convergence tolerances of the energy, gradient, and displacement are 10^{-5} Hartree, 2×10^{-3} Hartree/Å, and 5×10^{-3} Å, respectively. All electron DFT calculations in the present work are performed using a DMol³ package in the Materials Studio (version 5.5) [18−20] at the same level of theory except the different Monkhorst-Pack k points [21] used for the different supercell calculations.

It is known that the hybrid and the PBE+U methods can give better electronic properties. However, we need to choose different U and different hybrid functionals for different MnO₂ crystals as well as their sur-

_____

*Author to whom correspondence should be addressed. E-mail: weizg2003@126.com

711

faces. As a result, we can not compare the energies based on different calculation parameters as listed in Table I. Therefore, here we mainly list the results from PBE method as the calculations of Oxford *et al.* [15]. Some calculations are done with the PEB+U methods as listed in the supplementary material. It should be noted that the PBE+U methods gave the same conclusions about the MnO$_2$ structures, as presented in the later sections, such as the crash of α-MnO$_2$ and the small layer spacing of δ-MnO$_2$. Further studies about the optical properties, the conductivities, and the electronic structures are still needed for the MnO$_2$ system by the DFT+U and/or the hybrid methods.

III. RESULTS AND DISCUSSION

A. Calculations of α-MnO$_2$

The α-MnO$_2$ crystal structures can be found from XRD pattern JCPDS No.44-0141 with the lattice constants of $a=b=9.8521$ Å and $c=2.8647$ Å. When we calculated α-MnO$_2$ with the supercell Mn$_8$O$_{16}$ using the I4/m symmetry, the results were $a=b=9.8688$ Å and $c=2.8816$ Å, which agreed with the experimental results and the computational results of Cockayne *et al.* [22]. Whereas, when we calculated the same supercell without symmetry limit, it crashed as shown in Fig.1(a) (the crash also happened with the PBE+U methods as listed in the supplementary material). It is interesting because K$^+$ were visible in the X-ray experiment (JCPDS No.44-0141) and no α-MnO$_2$ has been synthesized without tunnel cations [13]. It means that K$^+$ should be in the supercell. So we added two K$^+$ cations to the supercell in the ideal tunnel cation positions such as $(0, 0, 0)$ and $(0.5, 0.5, 0)$, and calculated it again. There was no such crash in the supercell, the K$^+$ cations were still in their ideal position, their positive charges should be balanced by all the MnO$_6$ octahedrons in the tunnel and there was a small distortion in the MnO$_6$ octahedrons as shown in Fig.1(b). The symmetry of the optimized structure was close to I4/m and the lattice constants were $a=9.8410$ Å, $b=9.8939$ Å, and $c=2.9294$ Å, and the angles were $\alpha=\beta=90.0°$ and $\gamma=90.3°$. Then, we simulated the supercell with one K$^+$ in the ideal tunnel cation position $(0.5, 0.5, 0)$. The symmetry of the optimized structure was close to P4/m and the lattice constants were $a=9.9361$ Å, $b=9.8660$ Å and $c=2.9113$ Å, and the angles were $\alpha=\beta=\gamma=90.0°$. It is clear that K$^+$ cations would make the cell large and support the 2×2 tunnel without crashing. The larger lattice constants agreed with the X-ray results of natural minerals such as hollandite, cryptomelane, and priderite [23].

After the structure simulations, we calculated the formation ΔH [15, 24, 25] as the following

$$\Delta H=\left(E^{\mathrm{Mn}_x\mathrm{O}_y\mathrm{A}_z} - xE^{\alpha\text{-}\mathrm{Mn}} - y\frac{1}{2}E^{\mathrm{O}_2}-zE^{\mathrm{A}} \right)\frac{1}{x} \quad (1)$$
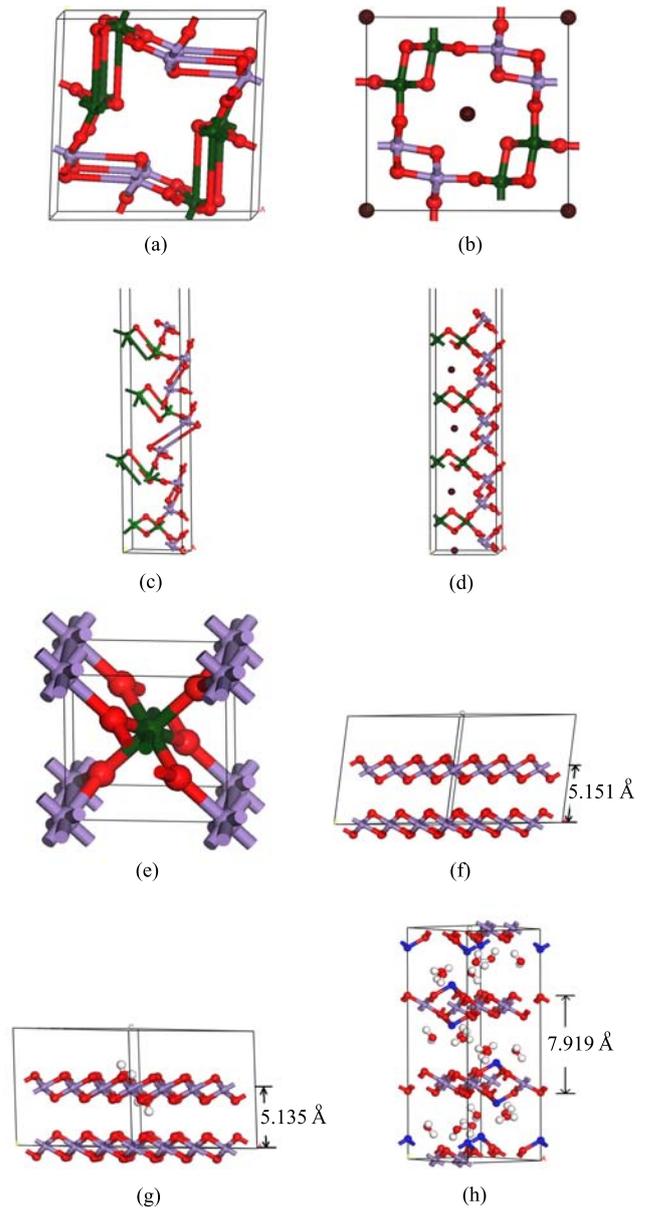

FIG. 1 The optimized MnO$_2$ crystals, where the O^{2-} ions are shown in red, the spin up and down Mn^{4+} cations are in lavender and green, the K$^+$, Zn^{2+}, and H$^+$ cations are in brown, blue and white, respectively. (a) The α-MnO$_2$ without metal cations, (b) the α-MnO$_2$ K$_{0.25}$MnO$_2$, (c, d) the (110) surface of α-MnO$_2$ without and with metal cations, (e) the β-MnO$_2$, (f) the defect free δ-MnO$_2$, (g) the defect δ-Mn$_{0.96875}$O$_2$H$_{0.125}$, and (h) the defect δ-Zn$_{0.25}$Mn$_{0.75}$O$_{1.75}$·0.75H$_2$O.

in which $E^{\mathrm{Mn}_x\mathrm{O}_y\mathrm{A}_z}$, $E^{\alpha\text{-}\mathrm{Mn}}$, E^{O_2}, and E^{A} were the DFT total energies for Mn$_x$O$_y$A$_z$, the α phase of bulk Mn, the oxygen molecule O$_2$ and the possible compositions in MnO$_2$ crystals such as K$^+$, Na$^+$, Ba^{2+}, respectively. x, y, z and the subscripts x, y, z denoted the number of Mn, O, and K, respectively. The DFT total energy of manganese metal was calculated for collinear anti-

TABLE I Comparison of the MnO$_2$ formation ΔH.

	ΔH/eV	
	Calculation results	Experimental results
α-MnO$_2$	-5.965 (K$_{0.25}$MnO$_2$)	-5.745 [13, 24] (K$_{0.3}$MnO$_2 \cdot$0.15H$_2$O)
	-5.601 (K$_{0.125}$MnO$_2$)	
β-MnO$_2$	-5.387 (MnO$_2$)	-5.387 [24] (Pyrolusite)
δ-MnO$_2$	-4.932 (MnO$_2$)	-6.100 [13, 24] (K$_{0.125}$MnO$_2 \cdot$0.19H$_2$O)
	-5.019 (Mn$_{0.96875}$O$_2$H$_{0.125}$)	
	-5.954 (Zn$_{0.25}$Mn$_{0.75}$O$_{1.75} \cdot$0.75H$_2$O)	
	-5.461 (Zn$_{0.25}$Mn$_{0.75}$O$_{1.75} \cdot$0.25H$_2$O)	

ferromagnetic (AFM) α-Mn using GGA optimized lattice constants as Hobbs *et al.* [26] and Oxford *et al.* [15] with the Monkhorst-Pack k points $4\times4\times4$ in the Mn$_{58}$ supercell [21]. For the DFT total energy of O$_2$, we added 0.451 eV per molecule to correct the overestimation from the DFT calculations [15, 24, 25, 27]. From Table I, the formation ΔH of K$_{0.25}$MnO$_2$ (calculated from K$_2$Mn$_8$O$_{16}$ supercell) was -5.965 eV, which was larger than that of -5.601 eV from K$_{0.125}$MnO$_2$ (calculated from KMn$_8$O$_{16}$ supercell). These results agreed with the experimental result of -5.745 eV for K$_{0.3}$MnO$_2 \cdot$0.15H$_2$O (with -5.387 eV in Ref.[24] and -34.5 kJ/mol in Ref.[13]) and the experimental trend that more metal cations could make the α-MnO$_2$ crystal more stable [13]. Based on these simulations we can explain that sufficient K$^+$ is an essential prerequisite for synthesis of the α-MnO$_2$ crystal [8].

The crash of α-MnO$_2$ also happened on its surface such as the (110) surface. When we simulated the surface without K$^+$ cations, the structure would crash as shown in Fig.1(c). When the K$^+$ cations were added, the surface would be stable as shown in Fig.1(d). It should be noted that we fixed the bottom layer and relaxed the top 3 layers with the supercell of K$_4$Mn$_{16}$O$_{32}$. When we added an oxygen molecule to this surface, the adsorption energy was 1.218 eV, the distance between the surface Mn^{4+} cation and O$_2$ was 2.2601 Å, the O$-$O bond of O$_2$ extended from 1.2423 Å to 1.2501 Å.

B. Calculations of β-MnO$_2$

When we used the Monkhorst-Pack k points $4\times4\times7$ in the β-MnO$_2$ supercell MnO$_2$O$_4$, the AFM state was found to be the ground state as shown in Fig.1(e), which was 108.7 and 543.0 meV per formula unit lower in energy than that of the ferromagnetic (FM) and nonmagnetic (NM) states, respectively. These magnetic results agreed with the experimental magnetic results [28] and the previous calculations from Oxford *et al.* [15], that the AFM state was 97 and 648 meV per formula unit lower in energy than that of the FM and NM states. At the same time, the optimized lattice constants of AFM β-MnO$_2$ such as a=4.4494 Å, b=4.4345 Å, c=2.8773 Å,

$\alpha=\beta=\gamma=90.0°$ were very close to the experimental results [29] a=b=4.4041 Å and c=2.8765 Å and the previous theoretical results [15] a=b=4.4569 Å and c=2.8823 Å.

Calculations about the β-MnO$_2$ crystal were done by different groups with the PBE, PBE0, B3LYP, HSE and PBE+U methods [15, 24, 30]. Detail comparisons between these methods were made by Franchini *et al.* [24] and Tompsett *et al.* [30]. Based on their calculations and our results, the standard PBE method used in the present work could give good optimized structures but a systematic correction was needed to evaluate the formation. The systematic error came from the calculations of MnO$_2$, α-Mn, and O$_2$, and this correction was applied in all the previous calculations [15, 24, 25]. Comparison of the formation from our PBE calculation with the experimental formation ΔH (-5.387 eV) in Ref.[24] indicated a correction of 0.451 eV per oxygen molecule. The 0.451 eV correction was smaller than that of 0.6, 0.90, and 1.15 eV in Refs.[24, 15, 25] respectively. In the present work, we took β-MnO$_2$ crystal as the benchmark for all the MnO$_2$ calculations, *i.e.*, 0.451 eV was applied to all the formation ΔH quoted, as listed in Table I.

C. Calculations of δ-MnO$_2$

The simulation results of the layer structure δ-MnO$_2$ are shown in Fig.1 (f) and (g). In 2008, Kwon *et al.* published the computational results about vacancy-free and Mn^{4+} defect δ-MnO$_2$ [31]. Their calculations provided the first direct evidence that such Mn^{4+} defects could indeed facilitate photoconductivity by reducing the band-gap energy and separating electron and hole states. Based on our calculations, we could also see that the Mn^{4+} defect could separate the electron and hole states, and reduce the band gap from 0.9 eV to 0.5 eV; these results were smaller than 1.3 eV to 0.9 eV from Kwon *et al.* [31]. However, there were still two differences. The first issue was about the lattice constant c (Kwon *et al.* fixed the $c/2$ to be 7.0005 Å [31]), even if the other lattice constants a and b were similar and the MnO$_2$ layer structures were almost the same.

From Fig.1 (f) and (g), the interlayer spacings ($c/2$) of the vacancy-free and defect MnO_2 with the supercells $Mn_{32}O_{64}$ and $Mn_{31}O_{64}H_4$ were 5.1505 and 5.1351 Å, respectively. It is known that the interlayer spacing could be tuned by incorporation of large molecules between the layers.

Post reported that the fresh Na-birnessite could change the interlayer spacing from 10 Å to 7 Å by drying and this process is irreversible [1]. They also proved that the large metal cations such as Ce cation could extend the interlayer spacing to 7.5135 Å [32]. Ching *et al.* reported that reactions between $NaMnO_4$ and glucose yielded two related Na-δ-MnO_2 products with 5.5 and 7 Å interlayer distances [33]. The 5.5 Å Na-δ-MnO_2 was identified as a dehydrated layered material which could be converted to 7 Å Na-δ-MnO_2 upon hydration. Based on these reports, the models in Fig.1 (f) and (g), which had no cations and water between the layers, should give a lower interlayer spacing than that of 5.5 Å from Ching *et al.* [33]. Therefore, the small interlayer spacings 5.1505 and 5.1351 Å should more closely agree with the experimental results. More tests about the interlayer spacing were made and listed in the supplementary material. It should be noted that the small interlayer spacings were confirmed for the δ-MnO_2 with different calculation methods. The second divergence was about the formation ΔH as listed in Table I. From Eq.(1) the formation ΔH of defect-free and defect δ-MnO_2 were -4.932 and -5.019 eV respectively, which were about 0.4 eV higher than that of -5.387 eV from β-MnO_2. However, Fritsch *et al.* reported that the formation ΔH of δ-MnO_2 were 0.713 eV lower than that of the β-MnO_2 at 298 K [13].

To achieve a deeper understanding of the structure and formation ΔH of δ-MnO_2, the hexagonal chalcophanite ($ZnMn_3O_7 \cdot 3H_2O$) was simulated with 6 units in one supercell as shown in Fig.1(h). The optimized lattice constants a and b were both 7.6042 Å, which were a little larger than that of the experimental results $a=b=7.533$ Å [29]. Whereas the interlayer spacing ($c/3$) 7.9192 Å was larger than that of the experimental result $c/3=6.931$ Å [34]. On the contrary, when there was less water in the model such as $ZnMn_3O_7 \cdot H_2O$, the interlayer spacing was 7.0780 Å, and the lattice constants a and b were 7.6617 and 7.6626 Å, respectively. The formation ΔH were -5.954 and -5.461 eV for $ZnMn_3O_7 \cdot 3H_2O$ and $ZnMn_3O_7 \cdot H_2O$, respectively as listed in Table I (the result of β-MnO_2 was -5.387 eV). These results agree with the experimental results that δ-MnO_2 are more stable than the β-MnO_2 at 298 K [13], and also support that the interlayer water is strongly bound to the interlayer cations, and plays an important role in the thermal stability of layered MnO_2 structures [14].

IV. CONCLUSION

In summary, based on the same kind of DFT method, different MnO_2 crystals such as α, β, δ-MnO_2 have been simulated. It was shown that metal cations as well as water were very important for the structural stability and energy stability of large tunnel structure α-MnO_2 (2×2 tunnel) and layer structure δ-MnO_2 (1×∞), therefore these factors can control the synthesis of manganese oxides. The importance of metal cations and water should be taken good care of during both the experiments and theoretical simulations.

Supplementary materials: The calculation results of MnO_2 by different computational methods such as PBE, PBE+U, *etc.* are given.

V. ACKNOWLEDGMENTS

[1] J. E. Post, Proc. Natl. Acad. Sci. USA **96**, 3447 (1999).
[2] J. E. Post and D. A. Mckeown, Am. Mineral. **86**, 701 (2001).
[3] Y. L. Lu, L. Yang, M. Wei, Y. Xie, and T. Liu, J. Solid State Electrochem **11**, 1157 (2007).
[4] O. Ghodbane, J. L. Pascal, and F. Favier, ACS Appl. Mater. Inter. **1**, 1130 (2009).
[5] C. Wang, L. Sun, Q. Q. Cao, B. Q. Hu, Z. W. Huang, and X. F. Tang, Appl. Catal. B **101**, 598 (2011).
[6] Q. Feng, H. Kanoh, and K. Ooi, J. Mater. Chem. **9**, 319 (1999).
[7] D. L. Zhao, X. Yang, H. Zhang, C. L. Chen, and X. K. Wang, Chem. Eng. J. **164**, 49 (2010).
[8] M. Sun, B. Lan, T. Lin, G. Cheng, F. Ye, L. Yu, X. L. Cheng, and X. Y. Zheng, CrystEngComm **15**, 7010 (2013).
[9] M. Sun, B. Lan, L. Yu, F. Ye, W. Song, J. He, G. Q. Diao, and Y. Y. Zheng, Mater. Lett. **86**, 18 (2012).
[10] B. Lan, M. Sun, T. Lin, G. Cheng, L. Yu, S. M. Peng, and J. Xu, Mater. Lett. **121**, 234 (2014).
[11] B. Lan, L. Yu, T. Lin, G. Cheng, M. Sun, F. Ye, Q. F. Sun, and J. He, ACS App. Mater. Inter. **5**, 7458 (2013).
[12] J. L. Zhou, L. Yu, M. Sun, F. Ye, B. Lan, G. Q. Diao, and J. He, J. Solid State Chem. **198**, 371 (2013).
[13] S. Fritsch, J. E. Post, S. L. Suib, and A. Navrotsky, Chem. Mater. **10**, 474 (1998).
[14] E. A. Johnson and J. E. Post, Am. Mineral. **91**, 609 (2006).
[15] G. A. E. Oxford and A. Chaka, J. Phys. Chem. **115**, 16992 (2011).

[16] J. P. Perdew and Y. Wang, Phys. Rev. B. **45**, 13244 (1992).

[17] N. A. Benedek, I. K. Snook, K. Latham, and I. Yarovsky, J. Chem. Phys. **122**, 144102 (2005).

[18] B. Delley, J. Chem. Phys. **92**, 508 (1990).

[19] B. Delley, J. Chem. Phys. **100**, 6107 (1996).

[20] B. Delley, J. Chem. Phys. **113**, 7756 (2000).

[21] H. J. Monkhorst and J. D. Pack, Phys. Rev. B **13**, 5188 (1976).

[22] E. Cockayne and L. Li, Chem. Phys. Lett. **544**, 53 (2012).

[23] J. E. Post, R. B. V. Dreele, and P. R. Buseck, Acta Cryst. B **38**, 1056 (1982).

[24] C. Franchini, R. Podloucky, J. Paier, M. Marsman, and G. Kresse, Phys. Rev. B **75**, 195128 (2007).

[25] D. A. Tompsett, S. C. Parker, and M. S. Islam, J. Am. Chem. Soc. **136**, 1418 (2014).

[26] D. Hobbs, J. Hafner, and D. Spišák, Phys. Rev. B **68**, 014407 (2003).

[27] S. Fritsch and A. Navrotsky, J. Am. Ceram. Soc. **79**, 1761 (1996).

[28] H. Sato, T. Enoki, M. Isobe, and Y. Ueda, Phys. Rev. B **61**, 3563 (2000).

[29] A. A. Bolzan, C. Fong, B. J. Kennedy, and C. J. Howard, Aust. J. Chem. **46**, 939 (1993).

[30] D. A. Tompsett, D. S. Middlemiss, and M. S. Islam, Phys. Rev. B **86**, 205126 (2012).

[31] K. D. Kwon, K. Refson, and G. Sposito, Phys. Rev. Lett. **100**, 146601 (2008).

[32] C. L. Lopano, P. J. Heaney, and J. E. Post, Am. Mineral. **94**, 816 (2009).

[33] S. Ching, D. J. Petrovay, M. L. Jorgensen, and S. L. Suib, Inorg. Chem. **36**, 883 (1997).

[34] J. E. Post and D. E. Appleman, Am. Mineral. **73**, 1401 (1988).